





Estimation of speed, armature temperature, and resistance in brushed DC machines using a CFNN based on BFGS BP

Hacene MELLAH^{1,2,*}, Kamel Eddine HEMSAS¹, Rachid TALEB², Carlo CECATI³

¹Department of Electrical Engineering, Faculty of Technology, Ferhat Abbas Sétif 1 University, Sétif, Algeria

²Department of Electrical Engineering, LGEER Laboratory, Faculty of Technology, Hassiba Benbouali University, Chlef, Algeria

³Department of Information Engineering, Computer Science, and Mathematics, University of L'Aquila, L'Aquila, Italy

Received: 25.11.2017

Accepted/Published Online: 20.10.2018

Final Version: 29.11.2018

Abstract: In this paper, a sensorless speed and armature resistance and temperature estimator for brushed (B) DC machines is proposed, based on a cascade-forward neural network and quasi-Newton BFGS backpropagation. Since we wish to avoid the use of a thermal sensor, a thermal model is needed to estimate the temperature of the BDC machine. Previous studies propose either nonintelligent estimators that depend on the model, such as the extended Kalman filter and Luenberger's observer, or estimators that do not estimate the speed, temperature, and resistance simultaneously. The proposed method has been verified both by simulation and by comparison with the simulation results available in the literature.

Key words: Cascade-forward neural network, parameter estimation, quasi-Newton BFGS, speed estimation, temperature estimation, resistance estimation

1. Introduction

In the last few years there has been growing interest in thermal aspects of electrical machines and their effects on electrical and mechanical parameters and time constants such as electrical resistance or back EMF [1], since, due to their influence, the motor's characteristics and hence its performance during operation are not the same as those considered during design [2]. Real-time knowledge of temperature in the various motor parts is also very useful in order to predict incipient failures and to adopt corrective actions, thus obtaining not only better control but also higher reliability of the electrical machine.

The early prediction of thermal aging, which makes insulations vulnerable, as well as of other thermal factors directly influencing motor health and life can avoid dangerous failures [3–5]. The main causes of thermal faults are overloads [6], cyclic mode [7], overvoltage and/or voltage unbalances [8], distortions [4], thermal insulation aging [3], obstructed or impaired cooling [9], poor design and manufacture [3], and skin effect [10].

For several years, great efforts have been devoted to the temperature and speed measurement of electrical machines, and several methods for temperature [11–13] and speed measurements [14] have already been proposed in the literature. While the direct measurement of temperature in electric DC machines is a long-established approach [13–15], some authors obtained the average winding temperature from the resistance measurement [13]. A more modern method can be found in [12,16], but the temperature measurement gave rise to two major

*Correspondence: h.mellah@univ-chlef.dz

problems: optimum sensor placement and the difficulty of achieving rotor thermal measurements. Likewise, speed measurement can also be difficult [17]. Moreover, information from sensors installed on rotating parts leads to techno-economic difficulties in the measurement chain. Sensorless solutions have therefore been considered by many studies [16,18–20].

One of the first examples of temperature estimation was presented in [21], where a Luenberger observer was applied both to a DC rolling mill motor and a squirrel cage induction motor. Another solution was described in [22], where the authors used a steady-state extended Kalman filter (EKF) associated with its transient version. To estimate the resistance some authors combine the EKF with a smooth variable structure filter [23]. Some research on bi-estimation has been done [24], which describes and implements an algorithm for combined flux-linkage and position estimation for PM motors based on the machine's characteristic curves. A very interesting approach was proposed in [25], applying and experimentally validating a transient EKF to estimate the speed and armature temperature in a BDC motor. However, the EKF has some limitations, in particular: (i) if the system is incorrectly modeled, the filter may quickly diverge; (ii) the EKF assumes Gaussian noise [26–28]; (iii) if the initial state estimate values are incorrect, the filter may also diverge; (iv) the EKF can be difficult to stabilize due to the sensitivity of the covariance matrices [27,29].

To the authors' knowledge, very few publications deal with the simultaneous estimation of speed and armature temperature of DC machines [25], especially when performed by intelligent techniques [29]. Artificial neural networks (ANNs) have demonstrated their ability in a wide variety of applications such as process control [30], identification [31], diagnostics [32], pattern recognition [33], robot vision [34], flight scheduling [35], finance and economics [36], and medical diagnosis [37].

In this paper, while referring to our previous study [29], in which an estimator based on a multilayer perceptron with Levenberg–Marquardt BP was developed in order to avoid the limitations of the standard ANN, a solution based on a cascade-forward neural network (CFNN) and Bayesian regulation BP (BRBP) is proposed. A highly accurate BRBP-based ANN was proposed in [38,39] but it requires an extremely long convergence time and is in fact known to be among the slowest algorithms to converge. Based on the approach already presented in [29], the purpose of this paper is to propose a novel approach using a learning algorithm that is a compromise between speed and accuracy. The BFGS can respond to these two constraints [39].

The remainder of the paper is organized as follows: Section 2 describes the thermal model of the BDC motor, Section 3 discusses the ANN and CFNN based on quasi-Newton BFGS BP, and Section 4 presents the simulation results and analysis. Finally, some conclusions are discussed in Section 5.

2. Thermal model of BDC machines

Research interest in studying rotating electric machinery from the combined viewpoints of thermal and electrical processes dates back to the 1950s [40,41]. The model used in this paper was proposed by Acarnley and Al-Tayie in [25]. This is a simplified model and is obtained by considering the power dissipation and heat transfer in the BDC machine [25]. The power is dissipated by the armature current flowing through the armature resistance, which varies in proportion to the temperature. The electrical equation of a BDC motor can be written as:

$$V_a = R_{a0} (1 + \alpha_{cu}\theta) i_a + L_a \frac{di_a}{dt} + k_e \omega \quad (1)$$

where V_a (V) is the armature voltage, R_{a0} (Ω) is the armature resistance at ambient temperature, α_{cu} (α_{cu} 0.004 1/ $^{\circ}$ C) is the temperature coefficient of resistance, θ ($^{\circ}$ C) the temperature above ambient, i_a (A) is the

armature current, L_a (H) is the armature inductance, k_e (V/rad/s) is the torque constant, and ω (rad/s) is the armature speed.

The mechanical equation of a BDC motor can be written as:

$$J \frac{d\omega}{dt} + b\omega + T_l = k_e i_a, \quad (2)$$

where J ($\text{kg} \times \text{m}^2$) is total inertia, b ($\text{N} \times \text{m} \times \text{s}$) is the viscous friction constant, and T_l ($\text{N} \times \text{m}$) is the load torque.

The power losses (P_l) include contributions from copper losses and iron losses, which are frequency-dependent; the copper loss is proportional to current squared multiplied by resistance, which depends on temperature, while the iron loss is proportional to speed squared for constant excitation multiplied by the iron loss constant ($k_{ir} = 0.0041 \text{ W}/(\text{rad/s})^2$) [25]:

$$P_l = R_{a0} (1 + \alpha_{cu} \theta) i_a^2 + k_{ir} \omega^2. \quad (3)$$

Heat flow from the armature surface of the BDC motor is directly to the cooling air and depends on the thermal transfer coefficients at zero speed ($k_o = 4.33 \text{ W}/^\circ\text{C}$) and at speed ($k_T = 0.0028 \text{ rad/s}$); the thermal power flow from the armature surface to the BDC motor surface is proportional to the temperature difference between the motor and the ambient temperature. The rate of temperature variation depends on the thermal capacity ($H = 18 \text{ KJ}/^\circ\text{C}$), and it was simplified by Acarnley and Al-Tayie in [25] as follows:

$$P_l = k_o (1 + k_T \omega) \theta + H \frac{d\theta}{dt}. \quad (4)$$

By arranging the previous equations, we can write the system of equations as follows.

$$\begin{aligned} \frac{di_a}{dt} &= -\frac{R_{a0}(1+\alpha_{cu}\theta)}{L_a} i_a - \frac{k_e}{L_a} \omega + \frac{1}{L_a} v_a \\ \frac{d\omega}{dt} &= \frac{k_e}{J} i_a - \frac{b}{J} \omega - \frac{K}{J} T_l \\ \frac{d\theta}{dt} &= \frac{R_{a0}(1+\alpha_{cu}\theta)}{H} i_a^2 + \frac{k_{ir}}{H} \omega^2 - \frac{k_o(1+k_T\omega)}{H} \theta \end{aligned} \quad (5)$$

3. ANN estimator

In recent years, CFNNs have become a widely used backpropagation algorithm [42–51] and have proved their capability in several applications [49–57]. CFNNs are similar to feedforward neural networks (FFNNs), but include a weight connection from the input to each layer and from each layer to the successive layers [49–56]. For example, a four-layer network has connections from layer 1 to layer 2, layer 2 to layer 3, layer 3 to layer 4, layer 1 to layer 3, layer 1 to layer 4, and layer 2 to layer 4. In addition, the four-layer network also has connections between input and all layers. FFNNs and CFNNs can potentially learn any input-output relationship, but CFNNs with more layers might learn complex relationships more quickly [50–53], making them the right choice for accelerated learning in ANNs [51]. The results obtained by Filik and Kurban in [52] suggest that CFNN BP can be more effective than FFNN BP in some cases.

In the present study, after solving Eq. (5), a random white Gaussian noise was added to the inputs and outputs of the BDC machine model. The outputs of the model were then used as the CFNN target and its inputs as the CFNN inputs, as shown in Figure 1. This noise makes the training very slow, but the CFNN is well trained and applicable in real time, and it is also used to track the performance and robustness of the

CFNN. Half of the simulation data of the BDC machine was used to create the training set and the other half was shared equally by the test and validation sets. The procedure used to train the NN was the cross-validation error checked over multiple sets of training data.

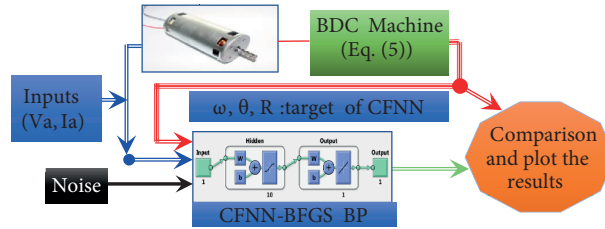


Figure 1. Estimating system of BDC machine by ANN based on BFGS BP.

The BP algorithm was used to form the neural network such that on all training patterns, the sum squared error (E) between the actual network outputs (y) and the corresponding desired outputs (y_d) was minimized to a supposed value:

$$E = \sum (y_d - y)^2. \tag{6}$$

To obtain the optimal network architecture, for each layer the transfer function types must be determined by a trial and error method. On the input (2 units) and three hidden layers (3, 4, and 5 units), a hyperbolic tangent sigmoid transfer function was used, defined as:

$$f(net_j) = \frac{2}{1 + e^{-2net_j}} - 1, \tag{7}$$

where net is the weighted sum of the input unit j , and $f(net)$ is the output units. The output layer has 3 units with a pure linear transfer function, defined as:

$$f(net_j) = net_j. \tag{8}$$

3.1. Quasi-Newton BFGS BP algorithm

The quasi-Newton BFGS BP training algorithm is a useful method for updating network weights and biases according to the BFGS formulae [58–61]. The algorithm belongs to the quasi-Newton family and was devised by Broyden, Fletcher, Goldfarb, and Shanno in 1970 [62–65] to achieve fast optimization [60,61]. It is an iterative method that approximates Newton’s method without the inverse of Hessian’s matrix [60]. It is a second-order optimization algorithm [60,61]. In this paper, the weight and bias values were updated according to the BFGS quasi-Newton method, and the new weight w_{k+1} was computed as:

$$w_{k+1} = w_k H_k^{-1} \Psi_k, \tag{9}$$

where H_k is the Hessian matrix of the performance index at the current values of the weights and biases. When H_k is large, w_{k+1} computation is complex and time-consuming [66–68]. BFGS does not calculate the inverse Hessian but approximates it as follows:

$$H_{k+1} = H_k + \frac{y_k y_k^T}{y_k^T S_k} \frac{H_k S_k S_k^T H_k}{S_k^T H_k S_k}, \tag{10}$$

where $\Psi_k = \nabla f(w_{k+1})$, $S_k = w_{k+1} - w_k$, and $y_k = \nabla f(w_{k+1}) - \nabla f(w_k)$. The new formula can be approximated as:

$$w_{k+1} = w_k \left(H_k + \frac{y_k y_k^T}{y_k^T S_k} - \frac{H_k S_k S_k^T H_k}{S_k^T H_k S_k} \right) \Psi_k. \quad (11)$$

This method has several advantages: it has a better convergence rate than using conjugate gradients [58–61], it is stable because the BFGS Hessian update is symmetric and positive definite [60], and BFGS computes an approximation to the inverse Hessian in only $O(n^2)$ operations [60]. However, this method requires a lot of memory to converge, especially on a large scale [66–69], whereas many researchers are interested in how to reduce memory needs [67–71].

4. Simulation results

Figures 2–5 show the simulation results of the simultaneous estimation of speed, armature temperature, and resistance by CFNN based on BFGS BP for continuous running duty or abbreviated by duty type S1. Duty type S1 is characterized by operation at a constant load maintained for a sufficient time to allow the machine to reach thermal equilibrium [72]. The ANN outputs are in good agreement with the model outputs as can be seen below, proving the ability of the proposed approach. The BDC motor parameters used during simulations are as follows:

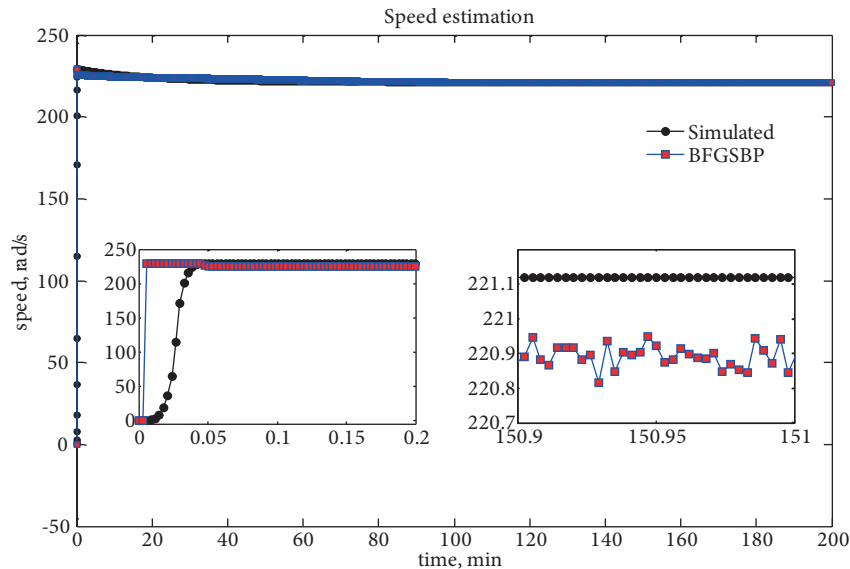


Figure 2. Estimated and simulated speed.

- Rated voltage $V_a = 240$ V
- Rated power $P = 3$ kW
- Rated torque $T_l = 11$ Nm
- Armature resistance $R_{a0} = 3.5$ Ω
- Armature inductance $L_a = 34$ mH

The estimated speed and the corresponding errors are shown in Figure 2. The results obtained by Acarnley and Al-Tayie in [25] suggest that the speed estimation error from the EKF is approximately 2%.

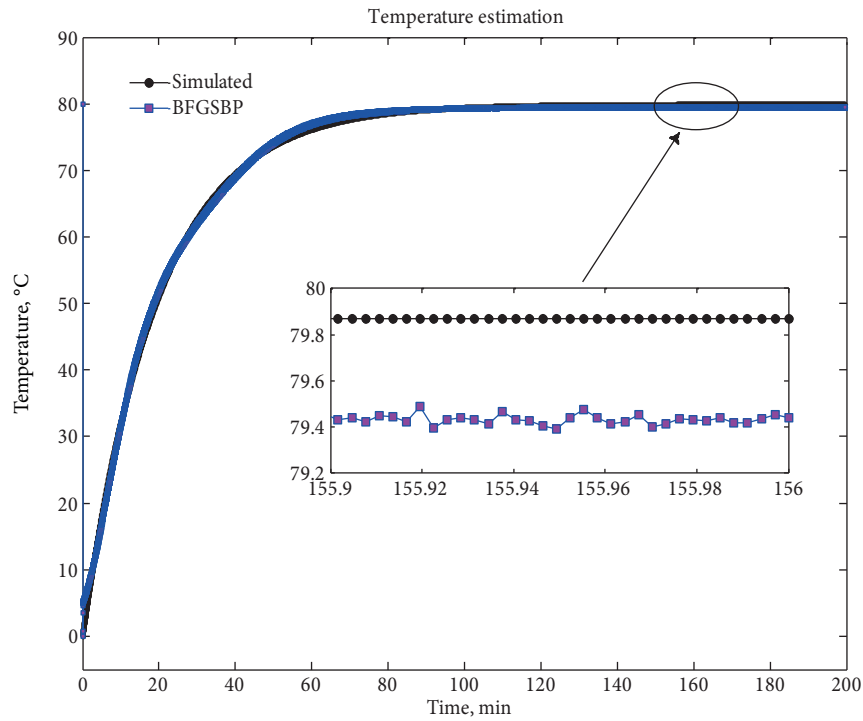


Figure 3. Estimated and simulated armature temperature.

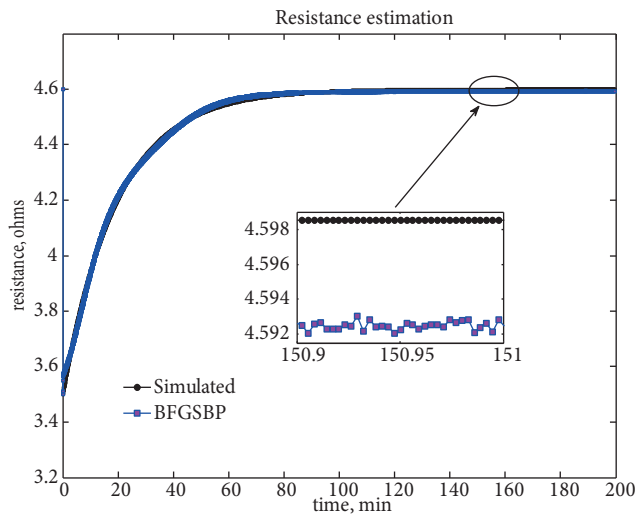


Figure 4. Estimated and simulated armature resistance.

Moreover, it is not suitable for high-performance servo drives [25]. However, in the results obtained here, the error is less than 0.4 rad/s and represents only 0.18% of the final value, as shown in Figure 5. The estimated temperature and the corresponding errors are shown in Figure 3, where it reaches 79.5 °C, while the model output is 80 °C and the steady state estimated error is less than 0.5 °C. This is insignificant and represents only 0.625%, as can be seen from Figures 3 and 5. This can be contrasted with the results in [25], which suggested that the temperature estimation error was 3 °C, i.e. approximately 3.75%, while Nestler and Sattler in [21]

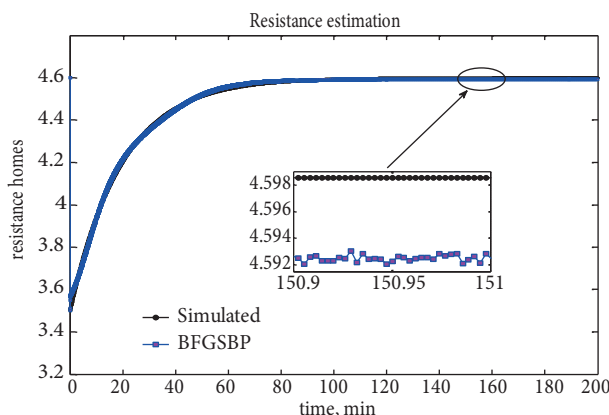


Figure 5. Speed, temperature, and resistance estimation errors.

found that the estimated winding temperature error was high. Even though Pantonial et al. in [22] reported an improvement, estimating that the error did not exceed $1\text{ }^{\circ}\text{C}$, the results presented in this paper are the best. Figure 4 depicts the resistance estimated by CFNN based on BFGS BP and the model response. It can be seen from this figure that the resistance has the same curvature as the armature temperature, where the steady state estimated resistance is $4.59\ \Omega$, i.e. less than 6×10^{-3} of the simulated resistance. Practically, this difference is a negligible quantity and represents only 0.13% of the final value. The results obtained are more precise than those presented in [23]. Figure 5 shows the estimation errors of speed, temperature, and resistance and their percentages in relation to their rated values. Figure 5 and the Table show more clearly the good agreement between the model outputs and the outputs of our intelligent sensor. The simulation results can be summarized by the Table.

Table. Summary of the estimation errors.

	$X_{model} - X_{Estimate}$	$(X_{model} - X_{Estimate})/X_{model}$
Speed	0.4 rad/s	0.18%
Temperature	0.5 $^{\circ}\text{C}$	0.625%
Resistance	0.006 Ω	0.13%

5. Conclusion

A sensorless simultaneous estimator for BDC machines based on a CFNN trained by BFGS BP has been proposed and verified through simulation and by comparison with earlier studies. The estimator includes sensorless speed estimation, average armature temperature, and resistance estimations based only on the voltage and the current measurements. Estimated speed and temperature eliminate the need for speed measurements and the need for a thermal sensor. In addition, estimated temperature solves the problem of obtaining thermal information from the rotating armature. Furthermore, the estimated temperature can be used for a new thermal monitoring method, motor protection, and other duty types since the model includes the load effect in the copper loss and the frequency effect in the iron loss. The estimated resistance can be used to improve the accuracy of the control algorithms that are affected by an increase in resistance as a function of temperature. Consequently, a sensorless simultaneous estimation of speed, temperature, and resistance could be a promising research field for future research. The good agreement between model and intelligent estimator results demonstrates the efficiency of the proposed approach.

References

- [1] Welch RHJ, Younkin GW. How temperature affects a servomotor's electrical and mechanical time constants. In: IEEE 2002 Industry Applications Conference, Conference Record of the 37th IAS Annual Meeting; 13–18 October 2002; Pittsburgh, PA, USA. New York, NY, USA: IEEE. pp. 1041-1046.
- [2] Ali SMN, Hanif A, Ahmed Q. Review in thermal effects on the performance of electric motors. In: 2016 International Conference on Intelligent Systems Engineering; 15–17 January 2016; Islamabad, Pakistan. New York, NY, USA: IEEE. pp. 83-88.
- [3] Stone GC, Culbert I, Boulter EA, Dhirani H. Electrical insulation for rotating machines. 2nd ed. New York, NY, USA: Wiley, 2004.
- [4] De Abreu JPG, Emanuel AE. Induction motor thermal aging caused by voltage distortion and imbalance: loss of useful life and its estimated cost. IEEE T Ind Appl 2002; 38: 12-20.
- [5] Grubic S, Aller JM, Lu B, Habetler TG. A survey on testing and monitoring methods for stator insulation systems of low-voltage induction machines focusing on turn insulation problems. IEEE T Ind Electron 2008; 55: 4127-4136.
- [6] Zocholl S. Understanding service factor, thermal models, and overloads. In: 59th Annual Conference for Protective Relay Engineers; 4–6 April 2006; College Station, TX, USA. New York, NY, USA: IEEE. pp. 141-143.
- [7] Valenzuela MA, Verbakel PV, Rooks JA. Thermal evaluation for applying TEFC induction motors on short-time and intermittent duty cycles. IEEE T Ind Appl 2003; 39: 45-52.
- [8] Gnaciński P. Windings temperature and loss of life of an induction machine under voltage unbalance combined with over-or under voltages. IEEE T Energy Conver 2008; 23: 363-371.
- [9] Zhang P, Du Y, Dai J, Habetler TG, Lu B. Impaired-cooling-condition detection using DC-signal injection for soft-starter-connected induction motors. IEEE T Ind Electron 2009; 56: 4642-4650.
- [10] Bonnett AH, Soukup GC. Cause and analysis of stator and rotor failures in three-phase squirrel-cage induction motors. IEEE T Ind Appl 1992; 28: 921-937.
- [11] IEEE. 119-1974, IEEE Recommended Practice for General Principles of Temperature Measurement as Applied to Electrical Apparatus. New York, NY, USA: IEEE 1975.
- [12] Yahoui H, Grellet G. Measurement of physical signals in rotating part of electrical machine by means of optical fibre transmission. Measurement 1997; 20: 143-148.
- [13] Compton FA. Temperature limits and measurements for rating of D-C machines. Transactions of the American Institute of Electrical Engineers 1943; 62: 780-785.
- [14] Bucci G, Landi C. Metrological characterization of a contactless smart thrust and speed sensor for linear induction motor testing. IEEE T Instrum Meas 1996; 45: 493-498.
- [15] AIEE. Temperature rise values for D-C machines: An AIEE committee report. Electrical Engineering 1949; 68: 581-581.
- [16] Ganchev M, Kral C, Oberguggenberger H, Wolbank T. Sensorless rotor temperature estimation of permanent magnet synchronous motor. In: 37th Annual Conference on IEEE Industrial Electronics Society; 7–10 November 2011; Melbourne, Australia. New York, NY, USA: IEEE. pp. 2018-2023.
- [17] Fiorucci E, Bucci G, Ciancetta F, Gallo D, Landi C, Luiso M. Variable speed drive characterization: review of measurement techniques and future trends. Adv Power Electron 2013; 2013: 968671.
- [18] Gao Z, Habetler TG, Harley R, Colby R. A sensorless rotor temperature estimator for induction machines based on current harmonic spectral estimation scheme. IEEE T Ind Electron 2008; 45: 407-416.
- [19] Gao Z, Habetler TG, Harley RG, Colby RS. A sensorless adaptive stator winding temperature estimator for mains-fed induction machines with continuous-operation periodic duty cycles. IEEE T Ind Appl 2008; 44: 1533-1542.
- [20] Acarnley PP, Watson JF. Review of position-sensorless operation of brushless permanent-magnet machines. IEEE T Ind Electron 2006; 53: 352-362.

- [21] Nestler H, Sattler PK. On-line-estimation of temperatures in electrical machines by an observer. *Electr Mach Power Syst* 1993; 21: 39-50.
- [22] Pantonial R, Kilantang A, Buenaobra B. Real time thermal estimation of a brushed DC motor by a steady-state Kalman filter algorithm in multi-rate sampling scheme. In: *IEEE TENCON 2012 Region 10 Conference*; 19–22 November 2012; Cebu, Philippines. New York, NY, USA: IEEE. pp. 1-6.
- [23] Zhang W, Gadsden SA, Habibi SR. Nonlinear estimation of stator winding resistance in a brushless DC Motor. In: *2013 American Control Conference*; 17–19 June 2013; Washington, DC, USA. New York, NY, USA: IEEE. pp. 4706-4711.
- [24] French C, Acarnley P. Control of permanent magnet motor drives using a new position estimation technique. *IEEE T Ind Appl* 1996; 32: 1089-1097.
- [25] Acarnley PP, Al-Tayie JK. Estimation of speed and armature temperature in a brushed DC drive using the extended Kalman filter. *IEE Proc Electr Power Appl* 1997; 144: 13-19.
- [26] Julier SJ, Uhlmann JK. New extension of the Kalman filter to nonlinear systems. In: *International Symposium on Aerospace Defense Sensing Simulation and Controls*; 21 April 1997; Orlando, FL, USA. Bellingham, Washington, USA: SPIE. pp. 182-193.
- [27] Bolognani S, Tubiana L, Zigliotto M. Extended Kalman filter tuning in sensorless PMSM drives. *IEEE T Ind Appl* 2003; 39: 1741-1747.
- [28] Peroutka Z, Šmídl V, Vošmik D. Challenges and limits of extended Kalman filter based sensorless control of permanent magnet synchronous machine drives. In: *13th European Conference on Power Electronics and Applications*; 8–10 September 2009; Barcelona, Spain. New York, NY, USA: IEEE. pp. 1-11.
- [29] Mellah H, Hemsas KE, Taleb R. Intelligent sensor based Bayesian neural network for combined parameters and states estimation of a brushed dc motor. *Int J Adv Comput Sci Appl* 2016; 7: 230-235.
- [30] Ahmad S, L. Khan. A self-tuning neurofuzzy feedback linearization-based damping control strategy for multiple HVDC links. *Turk J Elec Eng & Comp Sci* 2017; 25: 913-938.
- [31] Narendra KS, Parthasarathy K. Identification and control of dynamical systems using neural networks. *IEEE T Neural Networ* 1990; 1: 4-27.
- [32] Oyedotun O, Khashman A. Iris nevus diagnosis: convolutional neural network and deep belief network. *Turk J Elec Eng & Comp Sci* 2017; 25: 1106-1115.
- [33] Bishop CM. *Neural Networks for Pattern Recognition*. New York, NY, USA: Oxford University Press, 1995.
- [34] Shamsfakhr F, Sadeghibigham B. A neural network approach to navigation of a mobile robot and obstacle avoidance in dynamic and unknown environments. *Turk J Elec Eng & Comp Sci* 2017; 25: 1629-1642.
- [35] Kim BS, Calise AJ. Nonlinear flight control using neural networks. *J Guid Control Dynam* 1997; 20: 26-33.
- [36] Kaastra I, Boyd M. Designing a neural network for forecasting financial and economic time series. *Neurocomputing* 1996; 10: 215-223.
- [37] Bozkurt MR, Yurtay N, Yilmaz Z, Sertkaya C. Comparison of different methods for determining diabetes. *Turk J Elec Eng & Comp Sci* 2014; 22: 1044-1055.
- [38] Özer HM, Özmen A, Şenol H. Bayesian estimation of discrete-time cellular neural network coefficients. *Turk J Elec Eng & Comp Sci* 2017; 25: 2363-2374.
- [39] Afram A, Janabi-Sharifi F, Fung AS, Raahemifar K. Artificial neural network (ANN) based model predictive control (MPC) and optimization of HVAC systems: a state of the art review and case study of a residential HVAC system. *Energ Buildings* 2017; 141: 96-113.
- [40] Kaye J, Gouse SW. Thermal analysis of a small D-C Motor; Part I. Dimensional analysis of combined thermal and electrical processes. *Transactions of the American Institute of Electrical Engineers Part III* 1956; 75: 1463-1467.

- [41] Kaye J, Gouse SW, Elgar EC. Thermal analysis of a small D-C Motor; Part II. Experimental study of steady-state temperature distribution in a D-C Motor with correlations based on dimensional analysis. Transactions of the American Institute of Electrical Engineers Part III 1956; 75: 1468-1486.
- [42] Li W, Wu X, Jiao W, Qi G, Liu Y. Modelling of dust removal in rotating packed bed using artificial neural networks (ANN). Appl Therm Eng 2017; 112: 208-213.
- [43] Nabipour M, Keshavarz P. Modeling surface tension of pure refrigerants using feed-forward back-propagation neural networks. Int J Refrig 2017; 75: 217-227.
- [44] Venkadesan A, Himavathi S, Sedhuraman K, Muthuramalingam A. design and field programmable gate array implementation of cascade neural network based flux estimator for speed estimation in induction motor drives. IET Electr Power Appl 2017; 11: 121-131.
- [45] Sun C, He W, Ge W, Chang C. Adaptive neural network control of biped robots. IEEE T Syst Man Cyber: Syst 2017; 47: 315-326.
- [46] Saeedi E, Hossain MS, Kong Y. Side-channel information characterisation based on cascade-forward back-propagation neural network. J Electron Test 2016; 32: 345-356.
- [47] Taghavifar H, Mardani A, Taghavifar L. A hybridized artificial neural network and imperialist competitive algorithm optimization approach for prediction of soil compaction in soil bin facility. Measurement 2013; 46: 2288-2299.
- [48] Chayjan RA, Esna-Ashari M. Modeling isosteric heat of soya bean for desorption energy estimation using neural network approach. Chil J Agr Res 2010; 70: 616-625.
- [49] Lashkarbolooki M, Shafipour ZS, Hezave AZ. Trainable cascade-forward back-propagation network modeling of spearmint oil extraction in a packed bed using SC-CO₂. J Supercrit Fluid 2013; 73: 108-115.
- [50] Pwasong A, Sathasivam S. A new hybrid quadratic regression and cascade forward backpropagation neural network. Neurocomputing 2016; 182: 197-209.
- [51] Khaki M, Yusoff I, Islami N, Hussin NH. Artificial neural network technique for modeling of groundwater level in Langat Basin, Malaysia. Sains Malays 2016; 45: 19-28.
- [52] Filik UB, Kurban M. A new approach for the short-term load forecasting with auto-regressive and artificial neural network models. Int J Comput Intell Res 2007; 3: 66-71.
- [53] AL-Allaf ONA. Cascade-forward vs. function fitting neural network for improving image quality and learning time in image compression system. In: 2012 Proceedings of the World Congress on Engineering; 4-6 July 2012; London, UK. pp. 1172-1178.
- [54] Zhou YM, Meng ZJ, Chen XZ, Wu Z. Helicopter engine performance prediction based on cascade-forward process neural network. In: IEEE 2012 Conference on Prognostics and Health Management; 18-21 June 2012; Denver, CO, USA. New York, NY, USA: IEEE. pp. 1-5.
- [55] Lo Sciuto G, Cammarata G, Capizzi G, Coco S, Petrone G. Design optimization of solar chimney power plant by finite elements based numerical model and cascade neural networks. In: 2016 International Symposium on Power Electronics, Electrical Drives, Automation and Motion; 22-24 June 2016; Anacapri, Italy. New York, NY, USA: IEEE. pp. 1016-1022.
- [56] Hussain W, Hussain F, Hussain O. QOS prediction methods to avoid SLA violation in post-interaction time phase. In: IEEE 2016 11th Conference on Industrial Electronics and Applications; 5-7 June 2016; Hefei, China. New York, NY, USA: IEEE. pp. 32-37.
- [57] Serbest K, Bozkurt MR, Eldoğan O. Classification of cardiac arrhythmias with artificial neural networks according to gender differences. J Eng Sci Technol 2015; 10: 1144-1149.
- [58] Dao VNP, Vemuri R. A performance comparison of different back propagation neural networks methods in computer network intrusion detection. Differ Equations Dyn Syst 2002; 10: 1-7.

- [59] Mukherjee I, Routroy S. Comparing the performance of neural networks developed by using Levenberg-Marquardt and quasi-Newton with the gradient descent algorithm for modelling a multiple response grinding process. *Expert Syst Appl* 2012; 39: 2397-2407.
- [60] Becker S, Le Cun Y. Improving the convergence of back-propagation learning with second order methods. In: *Proceedings of the 1988 Connectionist Models Summer School; 17–26 June 1989; Los Angeles, CA, USA*. San Mateo, CA, USA: Morgan Kaufmann. pp. 29-37.
- [61] Saito K, Nakano R. Partial BFGS update and efficient step-length calculation for three-layer neural networks. *Neural Comput* 1997; 9: 123-141.
- [62] Broyden CG. The convergence of a class of double-rank minimization algorithms. *IMA J Appl Math* 1970; 6: 222-231.
- [63] Fletcher R. A new approach to variable metric algorithms. *Comput J* 1970; 13: 317-322.
- [64] Goldfarb D. A family of variable-metric methods derived by variational means. *Math Comput* 1970; 24: 23-23.
- [65] Shanno DF. Conditioning of quasi-Newton methods for function minimization. *Math Comput* 1970; 24: 647-647.
- [66] Apostolopoulou MS, Sotiropoulos DG, Livieris IE, Pintelas P. A memoryless BFGS neural network training algorithm. In: *IEEE 2009 7th International Conference on Industrial Informatics; Cardiff, UK*. New York, NY, USA: IEEE. pp. 216-221.
- [67] Zhao L, Wang D, Yang Y. The quadratic property of the L-MBFGS methods for training neural networks. In: *2011 International Conference on Mechatronic Science, Electric Engineering and Computer, Electric Engineering and Computer; 19–22 August 2011; Jilin, China*. New York, NY, USA: IEEE. pp. 849-852.
- [68] Bordes A, Pierre U. SGD-QN: careful Quasi-Newton stochastic gradient descent. *J Machine Learn Res* 2009; 10: 1737-1754.
- [69] Liu DC, Nocedal J. On the limited memory BFGS method for large scale optimization. *Math Program* 1989; 45: 503-528.
- [70] McLoone S, Irwin G. A variable memory quasi-Newton training algorithm. *Neural Process Lett* 1999; 9: 77-89.
- [71] Mokhtari A, Ribeiro A. Global convergence of online limited memory BFGS. *J Mach Learn Res* 2015; 16: 3151-3181.
- [72] IEC. IEC Publication 60034-1, Rotating Electrical Machines. Part 1: Rating and Performance. Geneva, Switzerland: IEC, 2004.